Stereo-Complex Crystallization of Poly(lactic acid)s in Block-Copolymer Phase Separation

Hiroki Uehara,* Yusuke Karaki, Shizuka Wada, and Takeshi Yamanobe

Department of Chemistry and Chemical Biology, Gunma University, Kiryu, Gunma 376-8515, Japan

ABSTRACT Block-copolymer containing a poly(L-lactic acid) (PLLA) segment was blended with pure poly(D-lactic acid) (PDLA) chain in chloroform solution and casted into the dried film. This method could form the stereocomplex (Sc) crystal of PLLA/PDLA within the nanometer-sized phase separation self-assembled by block-copolymer. Differential scanning calorimetry measurements of the prepared and annealed films gave the maximum achievable melting temperature of 245 °C, which was highest among those previously reported for PLA Sc-crystals. Surprisingly, all of added PDLA chains were Sc-crystallized, depending on the blend composition with block-copolymer containing PLLA.

KEYWORDS: poly(lactic acid) (PLA) • stereocomplex • block-copolymer • crystallization • melting

INTRODUCTION

The commercialized biomass-derived polymer poly(l-lactic acid) (PLLA) shows promise for the ideal carbon cycle excluding fossil resources. Since the melting temperature (T_m) of PLLA is relatively lower, at 170 °C, further improvement of the heat resistance of PLLA is still required especially for industrial applications. Therefore, the stereocomplex (Sc) crystalline form obtained by blending PLLA and poly(d-lactic acid) (PDLA) has received attention because of its higher T_m of 230 °C, as reported by frontier studies of Tsuji et al. (1−5). It is reported that an equimolar pair of PLLA and PDLA units is packed within this Sc-crystalline lattice (6−9). Various methods have been tried for enhancement of Sc-crystallization of PLA, including fiber spinning (10−14), drawing (15−17), annealing (18), polycondensation (19), in super critical carbon dioxide (20), or on surface (21). The higher T_m of Sc-form is especially useful for fabrics exposed by iron-press, such as shirts and shirtwaists.

In contrast, we focus on a microphase separation system self-assembled in block-copolymer material. Characteristic phase arrangements such as sphere, cylinder, or lamellar morphologies can be controlled by component ratios of counter blocks (22−24). If both PLLA and PDLA chains are combined within such a nanometer-sized microphase, Sc-crystallization is self-assembled. In this study, three materials were used. The first one was the diblock copolymer PLLA-*block*-polystyrene (PLLA-*b*-PS), composed of a PLLA block with a molecular weight (MW) of 1.95×10^4 and PS with an MW of 2.10×10^4. PLLA-*b*-PS has phase separation morphology typical of block-copolymers, reflecting a significant difference in the chain architecture of counter blocks (25). It has been reported that the same PLLA-*b*-PS composition exhibits typical lamellar morphology (26). The second material used in this study was PDLA homopolymer with an MW of 1.95×10^4, which was blended with the PLLA-*b*-PS in chloroform solution. Their blend ratio was adjusted in terms of PLLA and PDLA weight compositions (e.g., PLLA:PDLA is usually 50:50 or various weight compositions). For comparison, a controlled homopolymer blend composed of pure PLLA with an MW of 1.70×10^4 (the third material) and pure PDLA (the second material) was also prepared. The obtained polymer solutions were cast into films and the dried in vacuum at room temperature. These films were often annealed or molded at elevated temperatures. The obtained films were characterized by wide-angle X-ray diffraction (WAXD), differential scanning calorimetry (DSC), thermal gravimetry analysis (TGA), and scanning probe microscopy (SPM).

RESULTS AND DISUSSION

First, the crystalline forms of the prepared as-cast films were analyzed by WAXD measurements (see Figure S1 in the Supporting Information). The PLLA-*b*-PS/PDLA blend exhibited reflections attributed to the Sc-crystal lattice, which is usually obtained for a homopolymer blend of pure PLLA/PDLA. In contrast, the crystalline form of PLLA-*b*-PS alone was the typical α-form of homopolymer PLLA. Therefore, the melting behaviors of these different PLA systems were compared by DSC measurements. Figure 1a depicts the melting thermograms for PLLA-*b*-PS/PDLA blend (A) and homopolymer blend of pure PLLA/PDLA (B). For comparison, that for PLLA-*b*-PS alone (C) was also included. The glass transitions of PLLA and PS components appear at 60 and 100 °C. The PLLA-*b*-PS/PDLA blend exhibited double melting endotherms at 225 and 245 °C due to the melting of Sc-crystals. In contrast, a single endotherm at 170 °C was obtained for PLLA-*b*-PS alone, corresponding to the melting of the usual α-form crystal of PLLA. Such a high-temperature peak T_m of 245 °C was highest among those previously reported for PLA Sc-crystals. The sample degradation was characterized by TGA measurements, but only slight weight loss (<2%) starts above 250 °C for both PLLA-*b*-PS/PDLA

* Corresponding author. E-mail: uehara@chem-bio.gunma-u.ac.jp.
Received for review July 2, 2010 and accepted September 1, 2010

DOI: 10.1021/am1005755

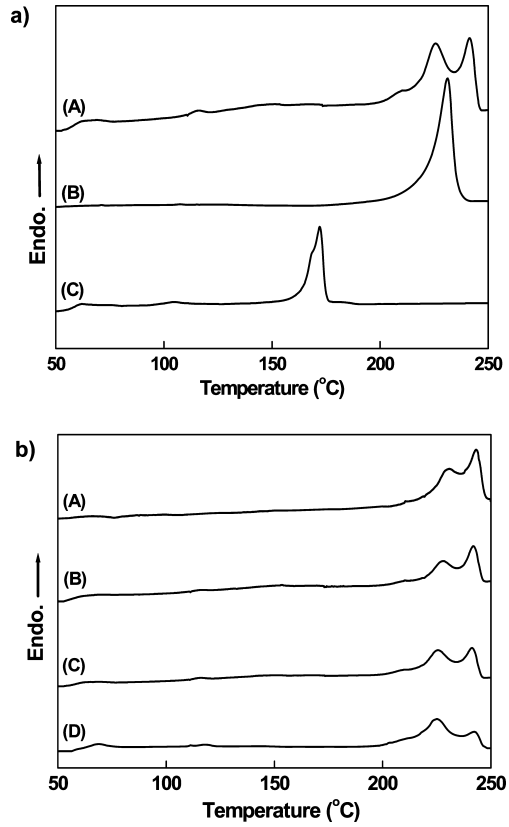

FIGURE 1. (a) Comparison of DSC melting thermograms for the as-cast films prepared from different PLA systems. PLLA-*b*-PS/PDLA blend with a PLLA:PDLA composition of 50:50 (A), homopolymer blend of pure PLLA and PDLA with a PLLA:PDLA composition of 50:50 (B), and PLLA-*b*-PS alone (C). Heating rate was 10 °C/min. The heat flow was normalized by total PLA weight composition. (b) Heating rate dependence of DSC melting thermograms for PLLA-*b*-PS/PDLA blend with a PLLA:PDLA composition of 50:50. (A) 2, (B) 5, (C) 10, and (D) 40 °C/min. The thermogram of A in a is the same as C in b.

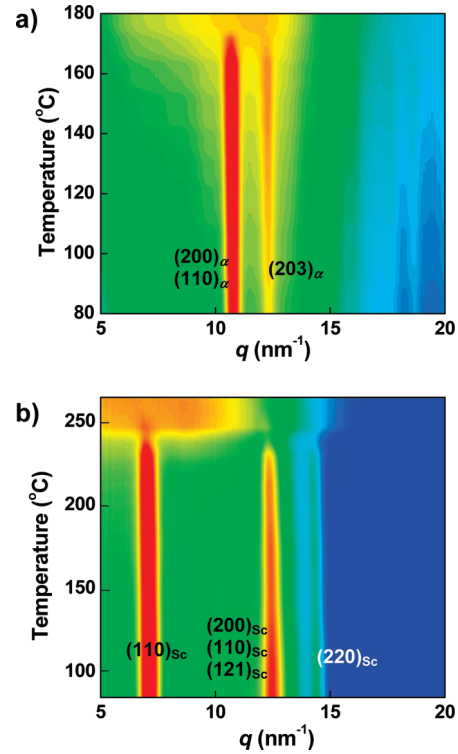

FIGURE 2. Duplicated WAXD line profiles recorded during heating for (a) PLLA-*b*-PS and (b) PLLA-*b*-PS/PDLA blend with a PLLA:PDLA composition of 50:50. The heating rate was 2 °C/min. Intensity is represented by a color gradation from blue (low) to red (high). The dimensional axis is represented by scattering vector $q = (4\pi\sin\theta)/\lambda$, where 2θ is the scattering angle and λ is the X-ray wavelength.

blend and PLLA-*b*-PS alone (see Figure S2 in the Supporting Information). Therefore, DSC double endotherm is attributed to the sample melting.

To clarify the origin of DSC double melting endotherms for the PLLA-*b*-PS/PDLA blend, the relationship between heating rate (*H.R.*) and endotherm shape was examined (Figure 1b). As *H.R.* increased, the high-temperature-side endotherm was reduced and the low-temperature-side endotherm was emphasized. Thus, low- and high-temperature-side endotherms result from the melting of the original Sc-crystals and those reorganized during DSC heating scan, respectively.

Such double melting behavior for PLLA-*b*-PS/PDLA blend film was also analyzed by X-ray measurements observed during heating. A higher luminescent synchrotron radiation source is effective for such in situ measurements, which require higher time resolution of data collection than usual ex situ measurements made at room temperature. Therefore, a custom-made heating chamber (27) was installed in a SPring-8 beamline, and a WAXD pattern was recorded during heating. Figure 2 depicts the changes in WAXD profiles with increasing temperature for PLLA-*b*-PS alone and the PLLA-*b*-PS/PDLA blend. The reflection intensity is represented by color gradation from low (blue) to high (red). For PLLA-*b*-PS, the reflection peaks of the usual α-form crystals disappeared at 170 °C, but those of Sc-crystals for the PLLA-*b*-PS/PDLA blend remained up to 245 °C. No reflection attributed to α-form was observed for the PLLA-*b*-PS/PDLA blend even at elevated temperatures up to complete melting. Peak intensities of these crystalline reflections rapidly decreased at 170 °C for PLLA-*b*-PS, because of the melting of α-form crystal, but exhibited a characteristic stepwise decrease at 225 and 245 °C for PLLA-*b*-PS/PDLA blend (see Figure S3 in the Supporting Information). Differential curves of these intensity changes demonstrated a single peak for PLLA-*b*-PS but double peaks for the PLLA-*b*-PS/PDLA blend, which coincide with DSC endotherms (Figure 1).

As indicated in Figure 1b, *H.R.* dependence on the DSC heating scan for the PLLA-*b*-PS/PDLA blend indicates that Sc-crystals can be reorganized at elevated temperatures before complete melting. Therefore, annealing at various temperatures was examined in the DSC pan for 30 min., and their DSC heating scans were compared (Figure 3a). The high-temperature-side endotherm gradually develops with increasing annealing temperature. For 225 °C annealing, the high-temperature-side endotherm becomes major, implying that reorganization of Sc-crystals is saturated. If this prediction is true, *H.R.* dependence is not recognizable for such annealed film. Indeed, the high-temperature-side endotherm was always larger, independent of *H.R* (see Figure S4 in the Supporting Information). Also, the positions of both low- and high-temperature-side endotherms were unchanged. These

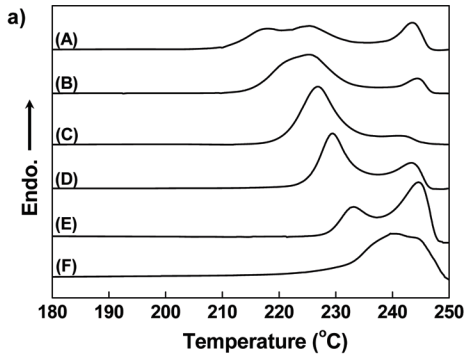

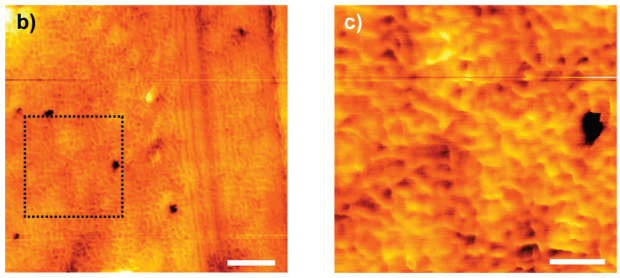

FIGURE 3. (a) Comparison of DSC melting thermograms of a series of PLLA-*b*-PS/PDLA blend film (PLLA:PDLA = 50:50) annealed under different temperatures: (A) 205 °C, (B) 210 °C, (C) 215 °C, (D) 220 °C, (E) 225 °C, and (F) 230 °C. Annealing time and *H.R.* were always 30 min and 10 °C/min. (b) SPM image of PLLA-*b*-PS/PDLA blend film (PLLA:PDLA = 50:50) annealed at 225 °C for 30 min. (c) Enlarged area depicted by the dotted square in b. Scale bars are (b) 250 and (c) 100 nm.

results indicate that reorganization with annealing is saturated at 225 °C, and this annealing condition is most effective for enhancement of high-temperature-side endotherm. Therefore, the morphology of the PLLA-*b*-PS/PDLA blend film annealed at 225 °C was observed by SPM scans with the tapping mode, which can detect the difference of phase arrangement in terms of surface stiffness for PLLA-*b*-PS morphology (28). It has been reported that the crystallization procedure affects the microphase separation even for PLLA-*b*-PS alone (29). Here, SPM phase image detects the difference in tapping response; therefore, PLA components composed of PLLA and PDLA segments reply the corresponding phase value. Thus, PLA components could be assigned to the larger fraction for 50:50 blend. In Figure 3, the area of the brighter region is larger than that of the darker one, meaning that the former is attributed to PLA components. The resultant phase image (Figure 3b,c) revealed networklike morphology induced by annealing, which is coincident with reorganization phenomenon of PLA phase as indicated by a series of DSC measurements described above. In contrast, the surface of as-prepared blend film is less flat; thus, the microphase separation morphologies could not be analyzed by SPM measurement.

Another characteristic of these thermograms for a series of annealed blend films is an appearance of the additional lowest-temperature endotherm for annealing below 210 °C. Indeed, similar endotherm was slightly observed for the unannealed blend film in Figure 1a(A), but more emphasized when annealing was applied. Therefore, this emdotherm is ascribed to melting of Sc-crystals formed during DSC heating

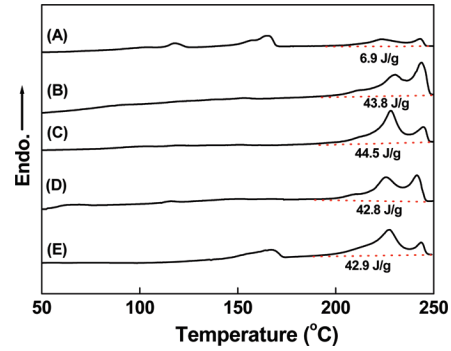

FIGURE 4. Comparison of DSC melting thermograms for a series of as-cast PLLA-*b*-PS/PDLA blend films with different PLLA:PDLA compositions of (A) 85:15, (B) 75:25, (C) 60:40, (D) 50:50, and (E) 25:75. Heating rate was 10 °C/min. The themogram of D is the same as that of A in Figure 1a. The indicated fusion heats were calculated with a weight basis of the total sample weight including all the components.

from amorphous PLLA and PDLA segments contained in as-prepared original blend film. However, their amount for the original blend film is very small, thus such cold-crystallization was unrecognizable for both DSC and in situ WAXD profiles in Figure 2b. For 215 °C annealing, this lowest-temperature endotherm becomes one component with previously mentioned lower-temperature-side endotherm. This phenomenon restricts reorganization of Sc-crystals during DSC scans, thus the higher-temperature-side endotherm was less recognized in Figure 3a(C). In contrast, annealing at 225 °C skips such cold-crystallization of amorphous PLA component, thus the higher-temperature-side endotherm develops on annealing. In such a case, the reorganization during DSC heating was not the origin of the higher-temperature endotherm, which was also confirmed from *H.R.* dependence (see Figure S4 in the Supporting Information).

When the peak positions of these endotherms originated from melting of Sc-crystals but with different thermal histories were plotted as annealing temperature in Figure S5 in the Supporting Information, the equilibrium melting temperature (T_m^o) could be estimated, according to Haffman-Weeks equation (30). Here, data sets of the lower-temperature-side T_m for double (not triple) endotherms were selected for T_m^o estimation of Sc-crystals formed in the 50:50 blend film. The resultant T_m^o was 247 °C, which was coincident with the observed T_m of the higher-temperature-side endotherm. This supports our assignment of the origin of the higher-temperature-side endotherm, namely, the equilibrium annealing is achieved on reorganization of original Sc-crystals.

Annealing below T_m of α-form of PLA was made at 100 and 150 °C, but almost same thermogram as the original blend film was obtained. Namely, there was no endotherm corresponding to melting of α-form crystal. In contrast, annealing beyond T_m of Sc-form at 250 °C gave only the low-temperature-side endotherm, but the Sc-crystallinity was remarkably reduced from the original one.

Characteristic melting behavior of blends with PLLA copolymer and pure PDLA also depends on blend compositions of PLLA:PDLA. Figure 4 depicts DSC melting thermograms for a series of PLLA-*b*-PS/PDLA blend films prepared

with different PLLA:PDLA compositions. Even with the much lower PDLA content for PLLA:PDLA = 85:15 blend (A), double melting endotherms of Sc-crystals appear above 225 °C. Another endotherm is also recognized at 170 °C, which is assigned to α-form melting. This α-form endotherm is similarly observed for PLLA:PDLA=25:75 blend (E) containing an excessive amount of homopolymer PDLA as a lone pair. However, it completely disappears when the PDLA composition increases until 75:25 (B). Here, the heat of melting (ΔH_m) for double endotherms of Sc-crystal melting was 44 J/g, which is similar to that for the 60:40 (C) and 50:50 blends (D). This situation is quite different from that for homopolymer blend having corresponding MW, where a 50:50 blend gives the highest ΔH_m (2). A 75:25 blend contains the lower amount of the equal unit pair of PLLA/PDLA; thus, Sc-form crystallinity normalized by such an equimolar portion could be achieved to 100%, assuming that the perfect heat of melting of Sc-crystal equals 155 J/g (9). This result indicates that all the PDLA homopolymer chains contribute to Sc-crystallization for this PLLA-*b*-PS/PDLA blend system. Such a highly crystalline state of Sc-form seems to be caused by enhanced chain contact within a limited nanometer-sized space originating from block-copolymer microphase separation. The reason of such constant ΔH_m value might be revealed by comparison of the in situ WAXD data for all of the blend ratios, but remains for future study.

Similar ΔH_m values for different blend compositions are unique melting characteristic for this blend system. Generally, sample $T_m = \Delta H_m/\Delta S_m$, where ΔS_m is the entropy of melting. The higher T_m for PLLA-*b*-PS/PDLA blend might be ascribed to the reduced ΔS_m for Sc-crystals because they are still confined in microphase separation of block copolymer after melting. Here, the order−disorder transition temperature of PLLA-*b*-PS having corresponding MW is over 300 °C (25). When the observed ΔH_m value for a 50:50 blend (43 J/g) was normalized by PLA composition, 65 J/g was obtained, corresponding to 42% Sc-crystallinity. This value was comparable to that for homopolymer blend (68 J/g), which is ascribed to the enhanced segmental motions for homopolymer chains with lower MW, compared to total copolymer chain length. This effect compensates Sc-crystallization for both cases, less spatial restriction on melting for homopolymer gave the resultant lower T_m.

In conclusion, a series of blends of PLLA-*b*-PS and PDLA homopolymer with PLLA:PDLA compositions from 75:25 to 50:50 could be effectively crystallized in Sc-form without the usual α-form. The obtained Sc-crystal for the blend exhibits a maximum achievable T_m at 245 °C. Also, double melting endotherms are characteristic for these blends, where reorganization of Sc-crystals occurs during heating scans. Surprisingly, all the PDLA chains contribute to Sc-crystallization, depending on the blend composition. Our PLA blend system composed of networks of Sc-crystals might be applicable to the heat-resistant materials, especially for automobiles, where practical usage of biomass-derivatives becomes social demand because fuel burning in engine necessarily releases the carbon dioxide gas.

Acknowledgment. Synchrotron WAXD measurements were performed at the BL40B2 in the SPring-8 with the approval of the Japan Synchrotron Radiation Research Institute (JASRI) (Proposal 2008A1148). We appreciate the cooperation of Drs. Hiroyasu Masunaga and Sono Sasaki (JASRI). This work was supported by Industrial Technology Research Grant Program from the New Energy and Industrial Technology Development Organization (NEDO) of Japan, and Grant-in-Aid for Scientific Research, The Ministry of Education, Culture, Sports, Science and Technology, Japan.

Supporting Information Available: Description of the experimental procedures, WAXD line profiles, TGA/DTA curves, WAXD intensity changes during heating for the different PLA systems, *H.R.* dependence for the annealed blend film, and Hoffman−Weeks plots of T_m vs T_a (PDF). This material is available free of charge via the Internet at http://pubs.acs.org.

REFERENCES AND NOTES

(1) Ikada, Y.; Jamshidi, K.; Tsuji, H.; Hyon, S.-H. *Macromolecules* **1987**, *20*, 904.
(2) Tsuji, H.; Hyon, S.-H.; Ikada, Y. *Macromolecules* **1991**, *24*, 5651.
(3) Tsuji, H.; Hyon, S.-H.; Ikada, Y. *Macromolecules* **1991**, *24*, 5657.
(4) Tsuji, H.; Ikada, Y. *Macromolecules* **1993**, *26*, 6918.
(5) Tsuji, H.; Ikada, Y. *Polymer* **1999**, *40*, 6699.
(6) Brizzolara, D.; Cantow, H.-J.; Diederichs, K.; Keller, E.; Domb, A. J. *Macromolecules* **1996**, *29*, 191.
(7) Tsuji, H.; Ikada, Y. *Macromol. Chem. Phys.* **1996**, *197*, 3483.
(8) Cartier, L.; Okihara, T.; Lotz, B. *Macromolecules* **1997**, *30*, 6313.
(9) Sawai, D.; Tsugane, Y.; Tamada, M.; Kanamoto, T.; Sungil, M.; Hyon, S.-H. *J. Polym. Sci., Part B: Polym. Phys.* **2007**, *45*, 2632.
(10) Tsuji, H.; Ikada, Y.; Hyon, S.-H.; Kimura, Y.; Kitao, T. *J. Appl. Polym. Sci.* **1994**, *51*, 337.
(11) Takasaki, M.; Ito, H.; Kikutani, T. *J. Macromol. Sci., Part B* **2003**, *42*, 403.
(12) Furuhashi, Y.; Kimura, Y.; Yoshie, N.; Yamane, H. *Polymer* **2006**, *47*, 5965.
(13) Tsuji, H.; Nakano, M.; Hashimoto, M.; Takashima, K.; Katsura, S.; Mizuno, A. *Biomacromolecules* **2006**, *7*, 3316.
(14) Ishii, D.; Ying, T. H.; Mahara, A.; Murakami, A.; Yamaoka, T.; Lee, W.; Iwata, T. *Biomacromolecules* **2009**, *10*, 237.
(15) Sawai, D.; Tamada, M.; Yokoyama, T.; Kanamoto, T.; Hyon, S.-H.; Moon, S. *Sen'i Gakkaishi* **2007**, *63*, 1.
(16) Sawai, D.; Tamada, M.; Kanamoto, T. *Polym. J.* **2007**, *39*, 953.
(17) Zhang, J.; Tashiro, K.; Tsuji, H.; Domb, A. J. *Macromolecules* **2007**, *40*, 1049.
(18) Fujita, M.; Sawayanagi, T.; Abe, H.; Tanaka, T.; Iwata, T.; Ito, K.; Fujisawa, T.; Maeda, M. *Macromolecules* **2008**, *41*, 2852.
(19) Fukushima, K.; Hirata, M.; Kimura, Y. *Macromolecules* **2007**, *40*, 3049.
(20) Purnama, P.; Kim, S. H. *Macromolecules* **2010**, *43*, 1137.
(21) Kakiage, M.; Ichikawa, T.; Yamanobe, T.; Uehara, H.; Sawai, D. *ACS Appl. Mater. Interfaces* **2010**, *2*, 633.
(22) Park, C.; Yoon, J.; Thomas, E. L. *Polymer* **2003**, *44*, 6725.
(23) Olson, D. A.; Chen, L.; Hillmyer, M. A. *Chem. Mater.* **2008**, *20*, 869.
(24) Wang, J.-Y.; Chen, W.; Russell, T. P. In *Unconventional Nanopatterning Techniques And Applications*; Rogers, J. A., Lee., H. H., Eds.; John Wiley & Sons: Hoboken, NJ, 2009; p 233.
(25) Ho, R.-M.; Chiang, Y.-W.; Chen, C.-K.; Wang, H.-W.; Hasegawa, H.; Akasaka, S.; Thomas, E. L.; Burger, C.; Hsiao, B. S. *J. Am. Chem. Soc.* **2009**, *131*, 18533.
(26) Chen, D.; Gong, Y.; Huang, H.; He, T.; Zhang, F. *Macromolecules* **2007**, *40*, 6631.
(27) Kakiage, M.; Sekiya, M.; Yamanobe, T.; Komoto, T.; Sasaki, S.; Murakami, S.; Uehara, H. *J. Phys. Chem. B* **2008**, *112*, 5311.
(28) Fu, J.; Wei, Y.; Xue, L.; Luan, B.; Pan, C.; Li, B.; Han, Y. *Polymer* **2009**, *50*, 1588.
(29) Ho, R.-M.; Lin, F.-H.; Tsai, C.-C.; Lin, C.-C.; Ko, B.-T.; Hsiao, B. S.; Sics, I. *Macromolecules* **2004**, *37*, 5985.
(30) Hoffman, J.; Weeks, J. J. *J. Res. Natl. Inst. Stand. Technol.* **1962**, *66A*, 13.

AM1005755